

Supporting Information

Fractality and Metastability of a Complex Amide Cross-linked Dipodal Alkyl/siloxane Hybrid

S. C. Nunes^{a,b*}, C. B. Ferreira^b, R. A. S. Ferreira^c, L. D. Carlos^c, M. C. Ferro^d, J. F. Mano^{e,f}, P. Almeida^a, V. de Zea Bermudez^{b,g*}

^aChemistry Department and CICS – Health Sciences Research Centre, University of Beira Interior, 6200-001 Covilhã.

^bChemistry Department, University of Trás-os-Montes e Alto Douro, 5000-801 Vila Real.

^cPhysics Department and CICECO, University of Aveiro, 3810-193 Aveiro, Portugal,

^dMaterials and Engineering Department and CICECO, University of Aveiro, 3810-193 Aveiro.

^e3B's Research Group – Biomaterials, Biodegradables and Biomimetics, University of Minho, Headquarters of the European Institute of Excellence on Tissue Engineering and Regenerative Medicine, AvePark, 4806-909, Taipas, Guimarães.

^fICVS/3B's - PT Government Associate Laboratory, Braga/Guimarães.

^gCQ-VR, University of Trás-os-Montes e Alto Douro, 5000-801 Vila Real.

Table of contents

Fig. S1 ^1H NMR spectrum of precursor P.	2
Fig. S2 ^{13}C CP/MAS (a) and ^{29}Si MAS (b) NMR spectra of hybrid A.	3
Table S1 ^{13}C CP/MAS and ^{29}Si MAS NMR data (δ in ppm) of hybrid A	4
Fig. S3 Picture of water droplet on the surface of a pestle of hybrid A confirming its hydrophobic nature.	
Fig. S4 EDS mapping of hybrid A: Si (c), C (d) and O (e).	5
Fig. S5 ATR/FT-IR (a) and FT-Raman (b) spectra of hybrid A in the $\nu_a\text{CH}_2$ and $\nu_s\text{CH}_2$ regions.	6
Fig. S6 FT-IR spectrum of hybrid A in the δCH_2 region.	7
Fig. S7 FT-Raman spectrum of hybrid A in the $\nu\text{C-C}$ region.	8
Fig. S8 Curve-fitting results performed in the amide I and amide II regions of hybrid A.	9
References	10

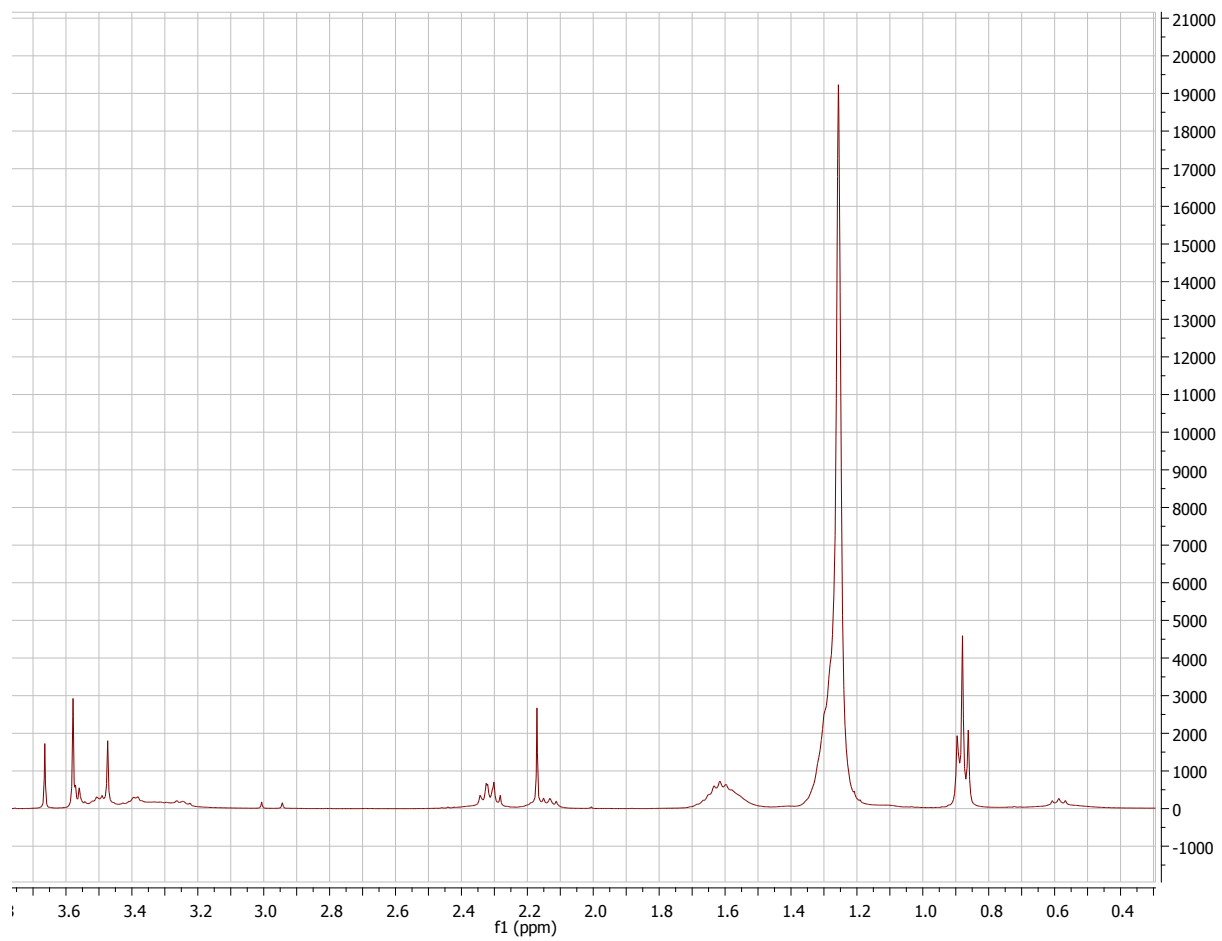


Fig. S1 ^1H NMR spectrum of precursor P.

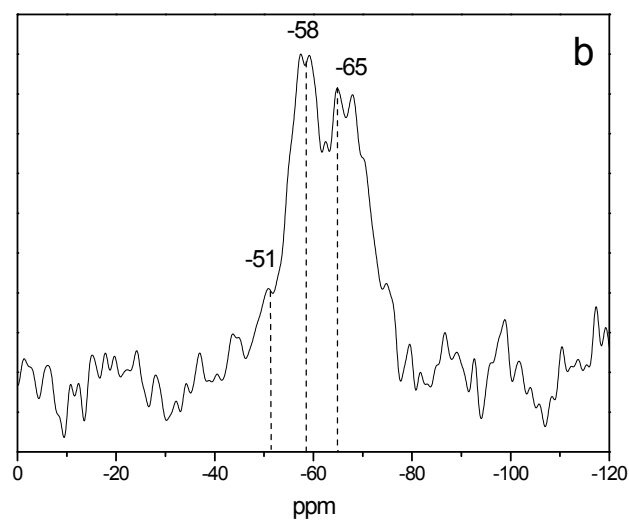
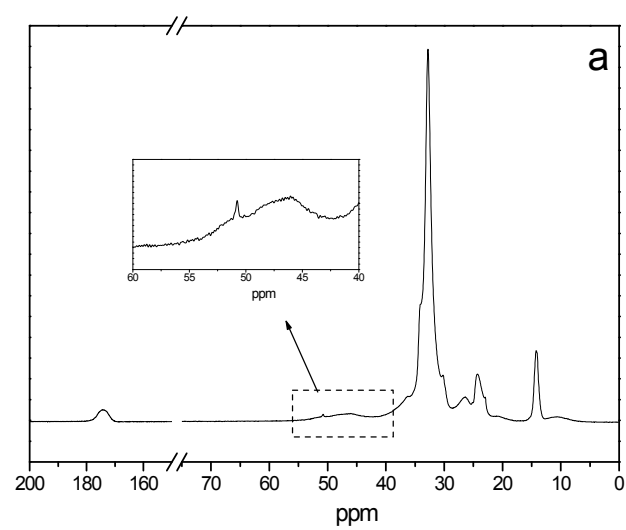


Fig. S2 ^{13}C CP/MAS (a) and ^{29}Si MAS (b) NMR spectra of hybrid A.

Table S1 ^{13}C CP/MAS and ^{29}Si MAS NMR data (δ in ppm) of hybrid A

^{13}C CP/MAS RMN		^{29}Si MAS RMN	
δ (ppm)	Attribution	δ (ppm)	Attribution
174.03	NHC(=O) and N <u>C</u> (=O)	-50.1 (5.6)	T^1 ($\text{CH}_2\text{-Si(OSi)(OR)}_2$) (area)
50.76	N <u>CH</u> ₂ and O <u>CH</u> ₃	-58.5 (48.2)	T^2 ($\text{CH}_2\text{-Si(OSi)}_2(\text{OR})$) (area)
36.53, sh	$\text{CH}_2\text{-C(=O)N}$, $\text{CH}_2\text{-C(=O)NH}$ and $\text{CH}_2\text{-NH-C(=O)}$	-68.2 (46.1)	T^3 ($\text{CH}_2\text{-Si(OSi)}_3$) (area)
34.10, sh		80	c
32.80	CH_2 <i>all trans</i> conformations	RSi(OR) _{0.5} (O) _{1.2}	Empirical Formula
30.00, sh	CH_2 <i>gauche</i> conformations		
26.40	CH_2		
24.43			
23.00	Si-CH ₂ CH ₂ and CH ₂ CH ₂ CH ₃		
14.00	CH ₂ CH ₃		
10.81	Si- CH ₂		

Notes: c (policondensation degree) = 1/3(A(T^1)+2A(T^2)+3A(T^3))*100

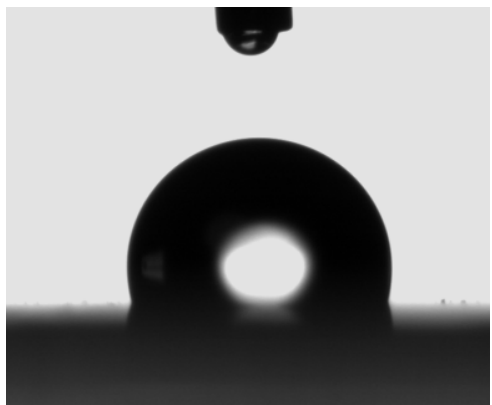


Fig. S3. Picture of water droplet on the surface of a pestle of hybrid A confirming its hydrophobic nature.

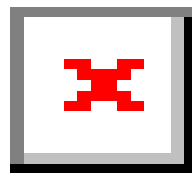
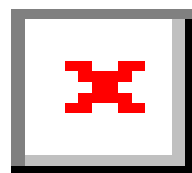
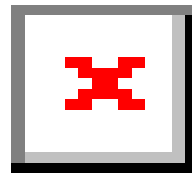
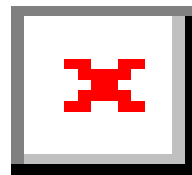
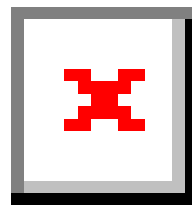


Fig. S4 EDS mapping of hybrid A: Si (c), C (d) and O (e).

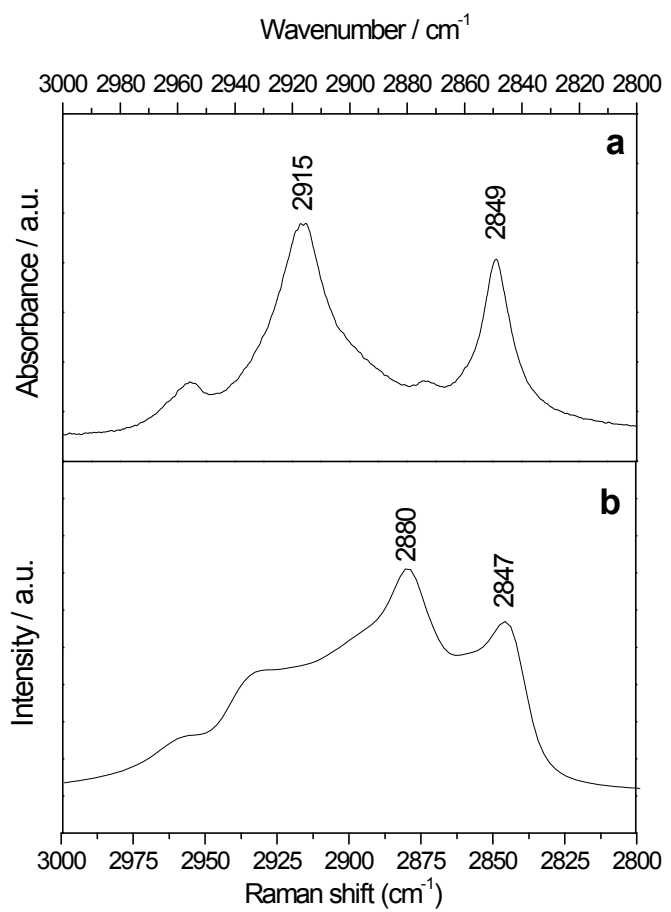


Fig. S5 ATR/FT-IR (a) and FT-Raman (b) spectra of hybrid A in the $\nu_a\text{CH}_2$ and $\nu_s\text{CH}_2$ regions.

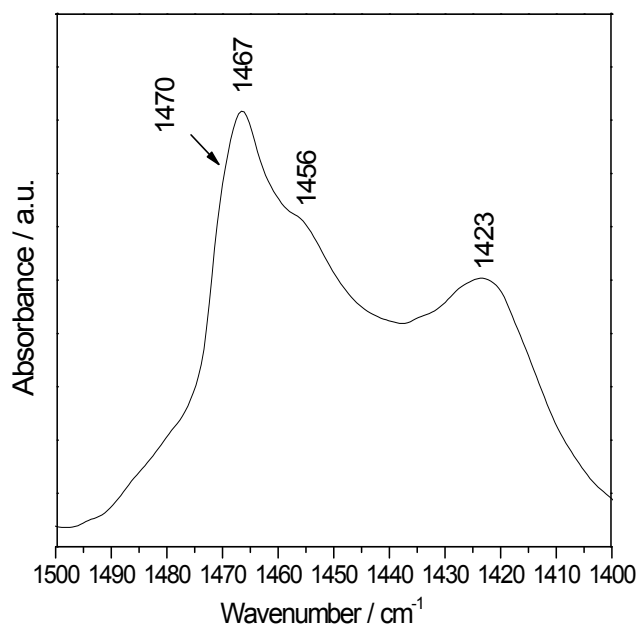


Fig. S6 FT-IR spectrum of hybrid A in the δCH_2 region.

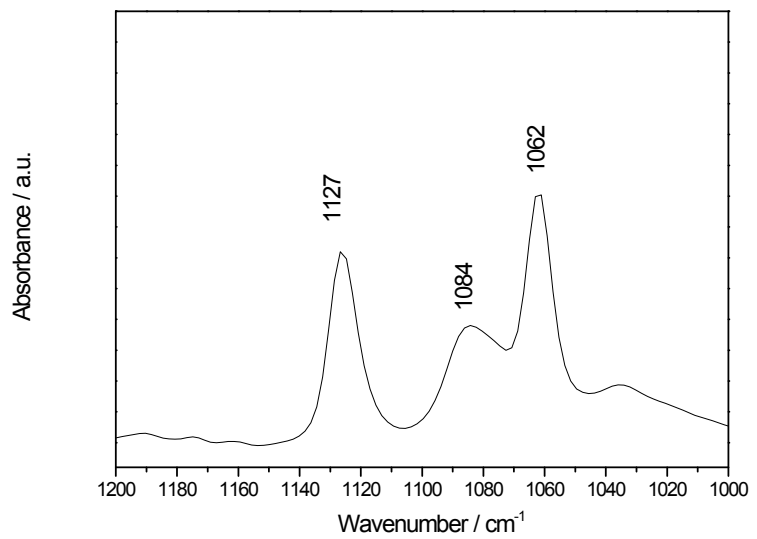


Fig. S7 FT-Raman spectrum of hybrid A in the vC-C region.

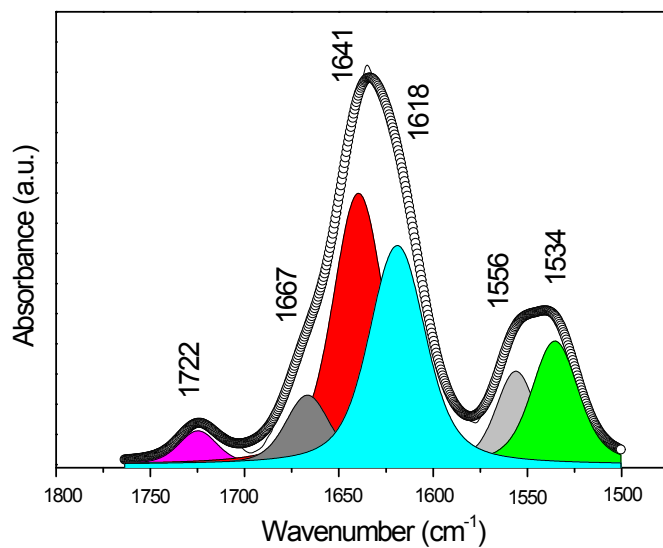


Fig. S8 Curve-fitting results performed in the amide I and amide II regions of hybrid A.